

1 Travel Behavior Classification: An Approach with Social 2 Network and Deep Learning

5 **Yu Cui**

6 Department of Civil, Structural and Environmental Engineering
7 University at Buffalo, The State University of New York
8 204 Ketter Hall, Buffalo, NY 14260
9 Phone: (716) 645-4351
10 Email: ycui4@buffalo.edu

13 **Qing He¹**

14 Department of Civil, Structural and Environmental Engineering and
15 Department of Industrial and Systems Engineering
16 University at Buffalo, The State University of New York
17 313 Bell Hall, Buffalo, NY 14260
18 Phone: (716)645-3470
19 Email: qinghe@buffalo.edu

21 **Alireza Khani**

22 Department of Civil, Environmental, and Geo-Engineering
23 University of Minnesota
24 500 Pillsbury Drive S.E.
25 Minneapolis, MN 55455
26 Phone: (612) 624-4411
27 Email: akhani@umn.edu

31 Submitted to TRB 97th Annual Meeting at Washington, D.C. January 2018
32 for Presentation and Publication

34 February 9, 2018

37 Word count: 4971 words text + (4 tables + 6 figures) x 250 words (each) = 7,471 words

¹ Corresponding Author

1 ABSTRACT

2 Uncovering human travel behavior is crucial for not only travel demand analysis but also
3 ridesharing opportunities. To group similar travelers, this paper develops a deep learning based
4 approach to classify travelers' behaviors given their trip characteristics, including time of day
5 and day of week for trips, travel modes, previous trip purposes, personal demographics, and
6 nearby place categories of trip ends. This study first examines the dataset of California
7 Household Travel Survey (CHTS) between the year of 2012 and 2013. After preprocessing and
8 exploring the raw data, we construct an activity matrix for each participant. The Jaccard
9 similarity coefficient is employed to calculate matrix similarities between each pair of
10 individuals. Moreover, given matrix similarity measures, we construct a community social
11 network for all participants. We further implement a community detection algorithm to cluster
12 travelers with similar travel behavior into the same groups. There are five clusters detected: non-
13 working people with more shopping activities, non-working people with more recreation
14 activities, normal commute working people, shorter working duration people, later working time
15 people, and individuals needing to attend school. We further build an image of activity map from
16 each participant's activity matrix. Finally, a deep learning approach with convolutional neural
17 network is employed to classify travelers into corresponding groups according to their activity
18 maps. The accuracy of classification reaches up to 97%. The proposed approach offers a new
19 perspective for travel behavior analysis and traveler classification.

20
21 *Keywords:* travel behavior; Jaccard similarity coefficient; community detection; convolutional
22 neural network in deep learning
23
24

1. INTRODUCTION

2 As car ownership inflates rapidly, together with increasing environmental concerns, we have
3 seen an increased interest in services that enable people to share their automobiles. Ride-sharing
4 or carpooling services are the ultimate way to make better use of the empty seats in personal
5 passenger cars in order to reduce fuel consumption, transportation cost, and emissions. Cici et al.
6 found that if individuals were willing to carpool with others who live and work within 1 km, the
7 traffic in the city of Madrid would decrease by 59% (1). There are many existing smartphone
8 apps providing the ride-sharing service. However, this kind of one-time sharing mode offers only
9 limited benefits. Long-time ride-sharing services can provide more advantages. There are many
10 kinds of travelers, including ones who depart at the same time of day, ones who do not have
11 regular departure times, ones who start work later than others, etc. Our assumption is that
12 travelers with the similar behaviors may enjoy their shared rides better given more common
13 behaviors. The long-term ride sharing matched according to travel behaviors will provide steady
14 benefits for transportation, environment, and society.

15 Household travel survey data, or travel itinerary data, is a major input to travel behavior
16 modeling. It can be used in many areas, particularly in travel behavior research and activity-
17 based travel demand forecasting. The traditional methods used for collecting these individual
18 travel data are telephone-based or computer-assisted interviews and activity logs recorded from
19 study participants. The typical drawbacks of these methods include high recruitment cost, low
20 response and sampling rates, undersampling or oversampling on certain types of trips,
21 inaccuracies in times, surrogate reporting and confusion of appropriate trip purpose (2).
22 Nowadays time-location data becomes accessible with the development of new techniques.
23 Travel activities can be traced by various sensors such as GPS, GSM, Wi-Fi, RFID, and
24 Bluetooth that are commonly available in smartphones or cars. Such data are usually collected
25 when an event is triggered such as making a phone call, passing a toll booth, or turning on
26 Bluetooth devices. Conducting a household travel survey with GPS devices is a complementary
27 way of collecting reliable and accurate data. GPS provides high-resolution time-space data. The
28 main advantages of the high-resolution GPS data include near-continuous location tracking, high
29 temporal resolution, and minimum report burden for participants, which may significantly
30 improve the understanding of travel activities in both spatial and temporal dimensions.

31 The essential goal of this study is to classify travelers based on the characteristics of their
32 historical travel data. Therefore, travelers within the same category could be potentially paired
33 and recommended with ride-sharing services. To pursue this goal, this paper constructs a social
34 network of travelers based on the Jaccard similarity coefficient, and employs a community
35 detection algorithm to cluster travelers into groups. In this paper, we borrow the concept from
36 social network to describe people who have similar behavioral patterns rather than construct a
37 real social network. After detecting travelers' groups, we manually assign labels to each group
38 according to trip and activity information. Further, we build an image of the activity map for
39 each traveler and employ a deep learning based approach to perform image classification.
40 Therefore, the travelers are classified accordingly into different groups depending on their
41 activity maps.

42 The rest of this paper is structured as follow: Section 2 summarizes previous studies in
43 travel behavior analysis, community detection and deep learning. Section 3 introduces the
44 datasets and initial result of the data analysis. Section 4 presents the methodology. Section 5
45 demonstrates the results with some numerical examples. Finally, Section 6 presents the
46 conclusions and future research.

2. LITERATURE REVIEW

2.1 Travel behavior data analysis and classification

Household trip data is crucial for travel demand forecasting and transportation system planning. The survey-based methods used for trip data collection went through the stages of paper and pencil interviews (PAPI), computer-assisted telephone interviews (CATI), and computer-assisted-self- interviews (CASI) (3). Although the computer-assisted interviews tried to help respondents to understand questions and recall trips they had during a day, these methods are restricted by the accuracy of recall, reliability, and compliance (4). Recently, GPS and GIS technologies have been used to supplement the traditional survey data. GPS and GIS land use data can be used for trip identification, travel characteristics identification, trip end clustering, trip purpose prediction (3; 5; 6). However, the accuracy is influenced by the dilution of precision of the GPS logs and inaccuracy in the GIS database (3). Kim et al. developed an activity travel data collection method facilitated by a smartphone application and an interactive web interface. The data collected this method in Singapore was further implemented with an ensemble-learning-based classification method to recognize travel patterns (7). Schumpeter et al. devised a multi-stage hierarchical matching procedure to calculate a cluster center of stop ends by combining trip ends and identifying trips with obvious purposes with the socio-demographics of the respondents (8). Some researchers also used decision tree based classifiers to derive trip purposes and implemented the methods in C4.5, C5.0, or an adaptive boosting environment (9; 10). Some of the previous studies above also require the social-economic characteristics of respondents (such as age, gender, and household income) for travel behavior analysis.

Researchers have also been making great efforts to classify travelers by using daily travel data and socio-demographic data. The criteria to select similarity measures depend on the analysts' importance ranking of various affecting attributes and the situations to be dealt with (11). Consequently, the resulting similarity measures could be subjective and case sensitive and thus derive quite inconsistent results. Hanson et al. divided individuals into five homogeneous travel behavior groups by using complex multi-day travel data and explained variability in individuals' daily travels (12). Shoval et al. implemented a sequence alignment method based on GPS data and clustered the data into three temporal-spatial time geographies (13). Kitamura and van der Horn showed that daily participation could be very stable in different types of activities (based on the categories of working, leisure, shopping and other activities) (14). Axhausen et al. collected six weeks' continuous travel diaries from about 300,000 inhabitants in Germany in Fall 1999 (15). Hazard models were used to analyze this high-quality data. A low degree of spatial variability of daily activities was also found from the analysis. Jiang et al. employed the K-Means algorithm via principal component analysis (PCA) to cluster daily patterns of human activities in Chicago (16). They separated more than 3000 individuals who participated in a 1-day or 2-day survey conducted by "Travel Tracker Survey" from January 2007 to February 2008 into 8 groups on weekdays and 7 groups on weekends, respectively. The same methodology applied to kernel density estimation, allowed them to analyze and explore diverse urban spatial-temporal structures. This research indicated how individuals in different activity pattern clusters make use of different sub-regions for different activity types (17). Travel behavior classification not only differentiates individuals with different travel patterns, but also uncovers human mobility patterns. Gonzalez et al. found that travel trajectories show lévy flight or random walk pattern to a large extent. Individuals show a high probability of returning to a few highly

1 frequented locations (18). This means humans are following highly predictable mobility patterns
2 (19). Ponieman et al. also retrieved social phenomena information (e.g. commute and major
3 sport events) from call detail records (CDR) data by just counting how many phone calls made
4 by users in two different time windows (from 9 p.m. to 5 a.m., and from 12p.m to 4 p.m. during
5 weekdays) from inside and outside Buenos Aires city. They found the average radius of
6 commute (ROC) was approximately 7.8 km (19). Nevertheless, that study was limited by the
7 accuracy of CDR data. With the combination of several machine learning algorithms, Ma et al.
8 identified travel patterns for transit riders from smart transit card data in order to attract more
9 users, retain loyal users, and finally improve overall transit services performance (20). Williams
10 et al. developed a new method derived from the neural coding concept of synchrony and
11 measured regularity of visiting a specific location for individuals (21). However, this research
12 only explored three places. It will provide more information to understand people travel patterns
13 if investigating how location types will influence visit patterns of individuals.
14

15 **2.2 Community detection**

16 Nowadays, lots of complex systems can be represented by networks. For instance, each user can
17 be a node in the social network. Then the friendship can be represented by edges. Researchers
18 aim to understand the network by finding community structures. A community is a collection of
19 nodes that are homogeneous within the group and heterogeneous with other groups in the
20 network, and this kind of network is known as a community structure. Newman and Girvan (22)
21 employed centrality indices to find boundaries of communities. They tested this method on two
22 networks which are collaboration networks and food web networks. Both cases retrieved
23 significant and informative community segments. The same authors also developed a community
24 detection algorithm and proposed a new community structure strength measurement(23). Their
25 algorithm showed highly effective performance for both computer-generated and real-world
26 networks while detecting communities. Radicchi et al. (24) developed a fully self-contained new
27 local algorithm for community detection and tested it on both artificial and real-world network
28 graphs. This new method demonstrated the potentials of implementing community detection
29 algorithms in large-scale technological and biological applications. In a community structure,
30 groups do not need to be necessarily mutually exclusive; they can overlap. Palla et al. (25)
31 proposed an algorithm which can uncover the overlapping community structure of complex
32 networks in nature and society. Community detection techniques can also be used for habitat
33 preservation, animal genetics and wildlife corridors (26). Moreover, it can be implemented in the
34 transportation field. For example, Lin et al. employed a community detection algorithm to study
35 vehicle accident causative factors (27).

36 Compared to traditional clustering algorithms, the community detection algorithm provides
37 several advantages. First, it is easy to implement, and steps are intuitive. Second, final networks
38 can be decomposed into communities for different levels. Third, this algorithm runs fast even for
39 large and high dimensional datasets.
40

41 **2.3 Deep learning**

42 With technological innovation, Artificial intelligence (AI) emerges and integrates into our
43 everyday life rapidly. From education to finance, from marketing to health care, and from
44 communication to transportation, with the advent of AI, individuals can save plenty of time,
45 reduce mistakes, relieve pressures, and stay safe (28).

1 Deep learning or deep neural network, as a branch of machine learning and AI, is an
2 artificial neural network (ANN) that contains more than one hidden layer. This kind of algorithm
3 has shown superior performance especially in automatic speech recognition, image recognition,
4 natural language processing, and recommendation systems. Readers can refer to Schmidhuber et
5 al. (29) for more details of deep learning. Deep neural networks typically can be categorized into
6 two types, recurrent neural networks (RNN) and convolutional neural networks (CNN). Long
7 short-term memory RNNs is a widely used algorithm in the field of speech recognition (30; 31).
8 However, in the field of image recognition, the convolutional neural network (CNN) is the most
9 prevailing algorithm. Krizhevsky et al. developed a CNN consisting of five convolutional layers,
10 some of these followed by max-pooling layers and three fully-connected layers. This network
11 achieved an error rate of 15.3% while implementing the ImageNet Large Scale Visual
12 Recognition Challenge (ILSVRC)-2012 dataset (32). Simonyan and Zisserman improved CNNs
13 with utilizing very small convolution filters and reached an error rate of 6.8% on the ILSVRC-
14 2014 dataset. He et al. won the ILSVRC-2015 competition with 3.57% error using deep residual
15 learning. Further, the winner team Trips-Soushen of ILSVRC-2016 produced a 2.99% error rate
16 (33; 34). This technique also has been applied in transportation, especially in the visual sensor
17 data (images, videos) processing domain. Only a few studies implemented deep learning in travel
18 behavior. Dong et al. employed deep learning to model driving behavior based on GPS data.
19 They combined CNN and RNN to extract features to represent driver behaviors. A driver
20 classification task was also conducted and they achieved significant outstanding performance
21 compared with traditional machine learning algorithms (35).

23 **3. DATA DESCRIPTION AND PRELIMINARY ANALYSIS**

24 In this paper, we acquire the raw data from the California Household Travel Survey (CHTS)
25 conducted by the California Department of Transportation (Caltrans) from February 2012 to
26 January 2013. The CHTS is designed to collect household travel information across all 58
27 counties of California and three adjacent counties in Nevada by using CATI, website, and GPS
28 devices. The entire household survey uses three types of GPS devices, wearable GPS device, in-
29 vehicle GPS device, and in-vehicle GPS device plus an on-board diagnostic (OBD) unit. There
30 are 108,778 individuals belongs to 42,431 households participated this survey in total, and
31 10,474 respondents from 5460 households carried GPS devices.

32 For households who conducted the survey with GPS devices, they will generate both
33 survey and GPS data. The survey data includes activities they completed on the assigned travel
34 date only. Each participant has one assigned travel date; this indicates that every participant only
35 has one day of survey data for both non-GPS households and GPS households. However, besides
36 survey data, GPS households also collect 7 days of GPS data as well.

37 There are 39 different trip purposes included in this household travel survey. We
38 categorize these trip purposes into 8 groups, which are home, work, school,
39 transportation/transitions (transit), shopping/errands (shop), personal business (person),
40 recreation/entertainment (rec), and other as shown in Table 1. Table 2 verifies the common
41 knowledge that there are more work and school activities during weekdays, while people have
42 more recreation, shopping, and personal business activities on weekends. It is found that the
43 average time individuals spend at home is 13.98 hours per day during weekdays and 16.77 hours
44 on weekends, respectively. The average time participants spend in the workplace is 7.11 hours
45 during the weekday and 5.51 hours on the weekend. Also, the average time that participants
46 spend at school is 5.18 hour during weekdays and 2.92 hours on weekends.

1 1. In this study, we only utilize data of participants who have both valid survey and GPS
 2 data. Several rules are created as follows in order to screen the feasible data. Both the first and
 3 last activity location should be 'home'.

4 2. Participants need to have more than one activity on the assigned travel date. If individuals
 5 stay at home for a whole assigned travel day, we cannot retrieve any travel information. This
 6 indicates that participants should also make more than 1 trip on the assigned travel date.

7 3. From the household survey data, we notice that there might be more than one driver
 8 utilizing the same vehicles within a household. It is difficult to distinguish travelers who share
 9 the same car since GPS trips are recorded at the vehicle level, not the person level. In order to
 10 avoid sampling errors arising from multiple drivers when they were sharing the same vehicle, we
 11 remove the records of the vehicles with multiple drivers.

12 After we apply these rules, 8849 unique individuals remain with 50,103 trips in this
 13 research. The radius of gyration (ROG) in transportation is a measure to describe the activity
 14 territory for each participant. According to Kang (36), we can calculate the ROG for each
 15 participant's trajectory up to time t by using the following formula:

$$16 \quad r_g^\alpha(t) = \sqrt{\frac{1}{n_c^\alpha(t)} \sum_{i=1}^{n_c^\alpha(t)} (x_i - x_c)^2 + (y_i - y_c)^2} \quad (1)$$

17 Where coordinates x_i, y_i denote the i th ($i = 1, 2, \dots, n_c^\alpha(t)$) position recorded for user α . And x_c
 18 and y_c represent the center of the mass of trajectories.

19 In Figure 1, the blue line is the ROG calculated for weekdays, and the red dashed line is
 20 the ROG for weekends. One can see that these two ROG distributions are almost the same.
 21 Therefore, individuals follow similar travel habits whether weekday or weekend. They seldom
 22 travel farther on weekends. Figure 1 also shows that there is a significant effect of distance
 23 decay. Moreover, based on the probability distribution of ROG, more than 95% of the
 24 participants have ROG values of less than 10 miles, and the mode is around 5 miles. This result
 25 is similar to the ROC calculated in Ponieman et al. (19) which is 7.8 km (4.85 miles).

26 Figure 2(a) and 2(b) depict the distribution of the first trip departure time and the last trip
 27 return time, respectively. As one can see, there is a significant pattern of departure time in the
 28 morning, and return time in the evening during weekdays. For weekends, individuals depart in
 29 the morning and return home in the evening later than weekdays. Moreover, the distribution of
 30 departure times on the weekend is flatter which means the departure times on the weekend
 31 involve more uncertainty than that on weekdays. The pattern of return time is similar. The mean
 32 first departure times on weekdays and weekends are 8:56 and 10:54, respectively. However, for
 33 the last trip return time, they are 18:28 and 17:55 for weekdays and weekends, respectively. As
 34 shown in Figure 2 (b), there is a small hump near noon. This hump is more flat and larger on
 35 weekends than weekdays. Individuals have more flexible times on weekends, and some of them
 36 may have eating, recreation, or shopping activities and return home at noon then stay home until
 37 the next day. On the contrary, individuals' departure and return times are restricted by work or
 38 study on weekdays.

40 4. METHODOLOGY

41 4.1 Matrix similarities

42 In this paper, we represent individuals' daily activities using a matrix. In order to construct this
 43 matrix, all activity purposes are categorized into 8 groups and 24 hours are divided into 288 five-
 44 minute bins. Therefore, the dimension of the matrix is 8x288. Each activity starts from the trip
 45 starting time for this activity and ends when the activity ends. For instance, an individual departs

1 from home at 5:30 pm to the supermarket, and arrives at the supermarket at 5:40 pm. This
 2 individual finishes shopping at 6:20 pm and leaves the supermarket. Therefore, this shopping
 3 activity is from 5:30 pm to 6:20 pm.

4 Individuals only can conduct one of 8 activities shown in Table 3 at one time. So,

$$5 x_{a,t} = \begin{cases} 1 & \text{when activity } a \text{ occurs at time interval } t \\ 0 & \text{otherwise} \end{cases} \quad (2)$$

6 where a represents activity and $a \in \{\text{Home, Work, School, Trans, Shop, Person, Rec, Other}\}$.
 7 t represents time bin number and $t \in [1, 288]$. In this fashion, a binary matrix is generated in
 8 order to represent daily activities. The two plots in Figure 3 are examples of color-coded daily
 9 activity matrices for two individuals. Figure 3(a) is a daily activity map of a student. This
 10 participant departs from home to school at approximately 7:30 a.m. and stay there until 2:30 p.m.
 11 After goes back home at 6:30 p.m., the student again attends a recreation activity, and returns
 12 home at 8:30 p.m.. Figure 3(b) describes a full time employee's weekday activities. The
 13 employee departs from home at 6:00 am, conducts a short personal business activity and a
 14 shopping trip after 6:00 pm off work.

15 Given individual's activity matrix, we now calculate the similarity between every pair of
 16 participants for constructing the community structure. In this paper, we implement the Jaccard
 17 similarity coefficient to measure similarities for binary matrices of individuals' daily trips.

$$18 J(A, B) = \frac{|A \cap B|}{|A \cup B|} = \frac{|A \cap B|}{|A| + |B| - |A \cap B|} = \frac{M_{11}}{M_{01} + M_{10} + M_{11}} \quad (3)$$

19 where A and B represents n binary entries, respectively. M_{01} represents the total number of
 20 entries where the entries of A is 0 and the entries of B is 1; M_{10} represents the total number of
 21 entries where the entries of A is 1 and entries of B is 0; M_{11} represents the total number of entries
 22 where the value of entries of A and B are both 1. Jaccard similarity coefficient ranges from 0 to
 23 1. If $J(A, B) = 0$, this means A and B are totally different. And if $J(A, B) = 1$, this means A and
 24 B are exactly the same. Moreover, if A and B are both empty, $J(A, B)$ is defined as 1.

25 Another similarity measure is the simple matching coefficient (SMC), shown in Equation
 26 (4). Unlike the Jaccard similarity coefficient, SMC includes M_{00} which represents the total
 27 number of entries where the entries of A and B are both 0. SMC is appropriate when 0 and 1
 28 represent equivalent information, such as gender (37). However, in this paper, 0 and 1 do not
 29 carry symmetrical information, and a majority of entries is 0 in the dataset. If we use SMC to
 30 measure similarity, M_{00} will dominate the similarity and force it close to 1. Therefore, the
 31 Jaccard similarity coefficient is more suitable to describe similarity for asymmetrical attributives
 32 than SMC.

$$33 SMC = \frac{M_{00} + M_{11}}{M_{00} + M_{01} + M_{10} + M_{11}} \quad (4)$$

35 4.2 Community detection

36 In this subsection, we first convert our data into a social network. Each participant in the dataset
 37 can be considered as a node. We use Jaccard similarity coefficient to measure the similarity
 38 between two users. If Jaccard similarity coefficient is greater than a threshold θ , it indicates two
 39 users have similar travel behaviors. In consequence, we create an edge between these two users.

$$40 \begin{cases} Edge_{ij} = 1 & W_{ij} \geq \theta \\ Edge_{ij} = 0 & W_{ij} < \theta \end{cases} \quad (5)$$

41 And the weight of the edge of user i and j can be represented by W_{ij} , this value equals to
 42 Jaccard similarity coefficient between these two users. After building the social network, we
 43 employ the fast unfolding community detection method to cluster nodes(38). This is a kind of

1 modularity maximization algorithm which is one of the most widely used methods for
 2 community detection.

3 In community detection, the modularity of a partition measures the density of edges
 4 within communities while comparing to edges between communities and scales between -1 and
 5 1. In the network where edges have weights, the formula of modularity is shown as following,

$$6 Q = \frac{1}{2m} \sum_{i,j} [W_{ij} - \frac{k_i k_j}{2m} \delta(c_i, c_j)] \quad (6)$$

7 where W_{ij} is the weight of the edge between node i and j ; $k_i = \sum_j W_{ij}$ represents the summation
 8 of the weights for edges attached to node i ; c_i is the community index assigned to this node in
 9 this iteration; $\delta(c_i, c_j)$ equals to 1 if $c_i = c_j$ and 0 otherwise; and $m = \frac{1}{2} \sum_j W_{ij}$.

10 This algorithm consists two stages. First, each node is assigned to different communities
 11 so that each node is a community, and the initial number of communities is as many as nodes.
 12 Then, for each node i , we measure the gains of modularity when removing i from its community
 13 and adding in neighboring communities respectively. Then for each isolated node i , we measure
 14 the gain of modularity when removing i from origin community and adding in neighboring
 15 communities respectively. And the node i will be allocated into the community with the maximal
 16 gain, but only if this gain is positive. If the maximum gain is not positive, node i will stay in
 17 original community. This stage will proceed recursively until a local maximum of the modularity
 18 is achieved. The second stage of this algorithm is to build a new network with communities
 19 found during the first part. After second stage is complete, we should reactivate the first stage of
 20 this algorithm to reconstruct weighted network. Then this two stages will run alternatively until
 21 there is no more changes and the global modularity maximum ($\max(q)$) is found.

23 **4.3 Deep learning**

24 Clustering procedure assigns same labels for individuals in same groups, and these labels are
 25 considered as the true label in the classification task. In order to classify travelers according to
 26 their activity maps, we implement the convolutional neural network (CNN) to complete this task.
 27 CNN, which is a kind of feed-forward artificial neural network, is recognized as a powerful and
 28 prevalent tool in image reorganization. Comparing to traditional neural network, CNN not only
 29 contains more layers, but also learn from filters, represented by a vector of weights with which
 30 we convolve the input. Filters are implemented to slide across all the areas of images, and the
 31 size of the commonly used filter is 2x2 which is also utilized in this paper. A CNN is composed
 32 of input and output layers, as well as multiple hidden layers between input and output layers.
 33 There are three kinds of hidden layers, including convolutional layers, pooling layers, and fully
 34 connected layers. The function of convolution layers is applying a convolution task to the input
 35 and pass the result to the next layer. Pooling layers combine the output from one layer and pass it
 36 into a single neuron in the other layer. In our CNN, every convolutional layer is followed by a
 37 pooling layer. Moreover, we implement the max pooling in the pooling layer which will pass the
 38 maximal value from the previous layer to the next layer. Fully connected layers aim to connect
 39 all neurons in the previous layer to all neurons in the next layer. Figure 4 illustrates a CNN with
 40 two convolutional layers and two fully connected layers. We construct this CNN in the next
 41 section.

42 In the traditional ANN networks, a sigmoid function is utilized to process data. However,
 43 in this paper, we implement Rectified Linear Units (ReLU), as shown below,

$$44 f(x) = \max(0, x) \quad (7)$$

45 where x is the input to a neuron.

1 The sigmoid function contains three problems: the first one is that saturated neurons kill the
 2 gradients that might always be zero. Second, the sigmoid output is not zero-centered. The last
 3 one is that the computation of exponential is very expensive. However, ReLU will not saturate
 4 in positive region and it is very computational efficient (approximately 6 times faster than
 5 sigmoid function) (32).

6 In this paper, the proposed CNN includes two fully connected layers, and this may result
 7 in overfitting since fully connected layer occupies most of the parameters. We add dropout
 8 process between two fully connected layers in order to prevent overfitting. Moreover, this
 9 process also can speed up the training process. Finally, we utilize cross entropy as the loss
 10 function as shown in equation 8.

11 $H(p, q) = -\sum_x p(x) \log q(x)$ (8)

12 where $p(x)$ and $q(x)$ are two probability distributions over discrete variable x , and $q(x)$ is the
 13 estimate distribution for true distribution $p(x)$. $H(p, q)$ is the cross entropy for the distribution p
 14 and q .

15 5. NUMERICAL EXAMPLES

16 In the first step, we construct a 1x2034 (=288x8) binary vector to represent the activity chain on
 17 the assigned travel date for each participant. Then we calculate the Jaccard similarity coefficient
 18 for every pair of individuals according to their activity matrices. The Jaccard similarity
 19 coefficient becomes the link weight between a pair of individuals. The Jaccard similarity
 20 coefficient ranges from 0 to 1. In this paper, we build an edge between two individuals in the
 21 community structure when the matrix similarity is greater than 0.9 ($\theta=0.9$). An undirected graph
 22 is constructed with 3887 nodes and 98026 edges, shown in Figure 5. We conduct an experiment
 23 to find an appropriate threshold θ of matrix similarity on 0.85, 0.9, and 0.95. When θ is 0.85,
 24 there are too many edges and the ratio of edge/node is too high. In this case, there is a very big
 25 cluster and several really small clusters. Therefore, the clustering result is not good for 0.85.
 26 When θ is set as 0.95, the number of the node is too low and the ratio of edge/node is too low as
 27 well. Each cluster contains not too many nodes. Moreover, most nodes are not clustered in any
 28 group. Therefore, the clustering result is not good for 0.95 neither. Under 0.90, the number of
 29 node, edge and edge/node is reasonable. The number of nodes within clusters is reasonable and
 30 there are significant differences among each cluster. Moreover, the number of nodes which do
 31 not belong to any cluster is not too high. Therefore, we set the threshold θ as 0.9. In this graph,
 32 we apply community detection algorithm with Gephi, a graph visualization tool. We finally
 33 detect 7 clusters in green (Cluster 1, 905 nodes), blue (Cluster 2, 229 nodes), pink (Cluster 3,
 34 1583 nodes), orange (Cluster 4, 255 nodes), red (Cluster 5, 172 nodes), and yellow (Cluster 6,
 35 147 nodes). The nodes isolated with others or not clustered in any groups are also displayed in
 36 the periphery in gray color, and they are considered as Cluster 7. Each node represents an
 37 individual, and nodes in same colors belong to the same clusters.

38 After identifying clusters, we summarize and conclude characteristics for each cluster.
 39 From Table 3, one can see that Cluster 1 and Cluster 2 represent individuals who do not go to
 40 work. On the contrary, individuals in Cluster 3, Cluster 4 and Cluster 5 need to work a lot. And
 41 participants in Cluster 6 spend lots of trip to school. Furthermore, Cluster 1 and Cluster 2 can be
 42 differentiated from each other according to shopping and recreation activities in Table 3. From
 43 Table 3, one can see that individuals in Cluster 1 conduct more shopping activities, whereas,
 44 individuals in Cluster 2 contains many more recreation activities. Then Cluster 3, Cluster 4, and
 45 Cluster 5 can be distinguished with the support of Figure 6. Figure 6 (a) shows the starting time

1 (including travel time) of first working activity. As one can see, individuals in Cluster 3 and
2 Cluster 4 go to work mostly at 7 am. However, the departure time of individuals in Cluster 5 is
3 much later and shows more uncertainty than individuals in other two clusters. Regarding Cluster
4 5, the departure time for the first working activity is distributed from 10 am to 2 pm more evenly.
5 To separate Cluster 3 and 4, we refer to Figure 6(b) that presents the working duration
6 distribution. One can see that Cluster 3 shows a high probability of working approximately 9
7 hours (including travel time to work) per day. However, for Cluster 4, the working duration,
8 which is around 5 hours, is much shorter than Cluster 3. The working duration distribution for
9 Cluster 5 is also flat and ranges from 4 to 12 hours.

10 In sum, individuals can be clustered into 7 groups:

- 11 • Cluster 1: Non-working individuals with more shopping activities
- 12 • Cluster 2: Non-working individuals with more recreation activities
- 13 • Cluster 3: Individuals with normal working start time and a full-time job
- 14 • Cluster 4: Individuals with part-time job
- 15 • Cluster 5: Individuals with late start working time
- 16 • Cluster 6: Individuals who need to attend school
- 17 • Cluster 7: Individuals that are not in any of the first 6 clusters

18 With identified travel behavior clusters, we perform a travel behavior classification task
19 with CNN to classify new travelers according to their activity maps. TensorFlow(39), one of
20 most powerful deep learning tools, is employed to construct CNN in this paper. According to
21 aforementioned clustering results, clusters have different sizes. In order to create a balance
22 training and testing datasets, we randomly select 100 records from each cluster for training, and
23 40 records from each cluster for test. There are 7 classes in classification task, in addition to the 6
24 classes which are identified by community detection algorithm, we add class ‘other’ which
25 represents users that are not in any of the 6 clusters. Moreover, we also implement several
26 traditional machine learning algorithms as benchmarks.

27 After training a CNN, we finally achieve accuracy as high as approximately 95% on the
28 test dataset, and detailed accuracy information for all algorithms are shown in Table 4.
29 Therefore, CNN is an appropriate and efficient algorithm for classifying participants into groups
30 with similar travel behavior according to their activity maps.

32 6. CONCLUSIONS

33 In this paper, we use California Household Travel Survey (CHTS) data to analyze and classify
34 travel behavior. After processing raw data, we find some interesting observations. First, travelers
35 make more commute trips to work and school during weekdays but more recreation, shopping,
36 and personal business activities on weekends. Second, most participants’ travel territory is
37 around 5 miles, and 95% of participants travel within 10 miles for each trip. Third, most
38 individuals have a low degree of spatial variability.

39 Based on 5-minute interval and 8 activity types, we further construct activity matrix for
40 each participant. Jaccard similarity coefficient is employed to calculate the similarity between
41 every pair of participants. The output similarities are utilized for constructing a social network
42 for participants. After this, we adopt a community detection algorithm to cluster individuals into
43 groups with same travel behavior. The algorithm produces seven clusters: (1) non-working
44 people with more shopping activities, (2) non-working people with more recreational activities,
45 (3) individuals with normal working start time and a full-time job, (4) Individuals with part-time
46 job, (5) individuals with late start working time, (6) individuals who need to attend school, and

(7) individuals that are not in any of the first 6 clusters. Then we classify individuals by using a CNN and achieve approximately 95% in accuracy.

In future, a variety of data sources, including passive trip trajectory data, transit smart card data, and social media data can be collected to provide more information about individual travel behavior. Therefore, the analysis of similar driver behavior can go a step further.

ACKNOWLEDGEMENT

This study was partially supported by National Science Foundation award CMMI-1637604 and Region 2 University Transportation Research Center faculty-initiated research project.

Author Contribution Statement

The authors confirm contribution to the paper as follows: study conception and design: Qing He, and Alireza Khani; data collection: Yu Cui; analysis and interpretation of results: Yu Cui, Qing He, and Alireza Khani; draft manuscript preparation: Yu Cui, Qing He, and Alireza Khani. All authors reviewed the results and approved the final version of the manuscript.

REFERENCE

- [1] Cici, B., A. Markopoulou, E. Frias-Martinez, and N. Laoutaris. Assessing the potential of ride-sharing using mobile and social data: a tale of four cities. In *Proceedings of the 2014 ACM International Joint Conference on Pervasive and Ubiquitous Computing*, ACM, 2014. pp. 201-211.
- [2] Gong, L., T. Morikawa, T. Yamamoto, and H. Sato. Deriving personal trip data from GPS data: a literature review on the existing methodologies. *Procedia-Social and Behavioral Sciences*, Vol. 138, 2014, pp. 557-565.
- [3] Wolf, J., R. Guensler, and W. Bachman. Elimination of the travel diary: Experiment to derive trip purpose from global positioning system travel data. *Transportation Research Record: Journal of the Transportation Research Board*, No. 1768, 2001, pp. 125-134.
- [4] Wu, J., C. Jiang, D. Houston, D. Baker, and R. Delfino. Automated time activity classification based on global positioning system (GPS) tracking data. *Environmental Health*, Vol. 10, No. 1, 2011, p. 101.
- [5] Bohte, W., and K. Maat. Deriving and Validating Trip Destinations and Modes for Multiday GPS-Based Travel Surveys: Application in the Netherlands. In *Transportation research board 87th annual meeting*, 2008.
- [6] Chen, C., H. Gong, C. Lawson, and E. Bialostozky. Evaluating the feasibility of a passive travel survey collection in a complex urban environment: Lessons learned from the New York City case study. *Transportation Research Part A: Policy and Practice*, Vol. 44, No. 10, 2010, pp. 830-840.
- [7] Kim, Y., F. C. Pereira, F. Zhao, A. Ghorpade, P. C. Zegras, and M. Ben-Akiva. Activity recognition for a smartphone and web based travel survey. *arXiv preprint arXiv:1502.03634*, 2015.
- [8] Schönenfelder, S., K. W. Axhausen, N. Antille, and M. Bierlaire. Exploring the potentials of automatically collected GPS data for travel behaviour analysis. 2002.
- [9] Deng, Z., and M. Ji. Deriving rules for trip purpose identification from GPS travel survey data and land use data: A machine learning approach. In *Traffic and Transportation Studies 2010*, 2010. pp. 768-777.
- [10] Griffin, T., and Y. Huang. A decision tree classification model to automate trip purpose derivation. In *The Proceedings of the ISCA 18th International Conference on Computer Applications in Industry and Engineering*, 2005. pp. 44-49.
- [11] Jones, P. Developments in dynamic and activity-based approaches to travel analysis. *Oxford Studies in Transport*, 1990.

[12] Hanson, S., and J. Huff. Classification issues in the analysis of complex travel behavior. *Transportation*, Vol. 13, No. 3, 1986, pp. 271-293.

[13] Shoval, N., and M. Isaacson. Sequence alignment as a method for human activity analysis in space and time. *Annals of the Association of American geographers*, Vol. 97, No. 2, 2007, pp. 282-297.

[14] Kitamura, R., and T. Hoorn. Regularity and irreversibility of weekly travel behavior. *Transportation*, Vol. 14, No. 3, 1987, pp. 227-251.

[15] Axhausen, K. W., A. Zimmermann, S. Schönsfelder, G. Rindsfüser, and T. Haupt. Observing the rhythms of daily life: A six-week travel diary. *Transportation*, Vol. 29, No. 2, 2002, pp. 95-124.

[16] Jiang, S., J. Ferreira, and M. C. González. Clustering daily patterns of human activities in the city. *Data Mining and Knowledge Discovery*, 2012, pp. 1-33.

[17] Jiang, S., J. Ferreira Jr, and M. C. Gonzalez. Discovering urban spatial-temporal structure from human activity patterns. In *Proceedings of the ACM SIGKDD international workshop on urban computing*, ACM, 2012. pp. 95-102.

[18] Gonzalez, M. C., C. A. Hidalgo, and A.-L. Barabasi. Understanding individual human mobility patterns. *Nature*, Vol. 453, No. 7196, 2008, pp. 779-782.

[19] Ponieman, N. B., A. Salles, and C. Sarraute. Human mobility and predictability enriched by social phenomena information. In *Proceedings of the 2013 IEEE/ACM International Conference on Advances in Social Networks Analysis and Mining*, ACM, 2013. pp. 1331-1336.

[20] Ma, X., Y.-J. Wu, Y. Wang, F. Chen, and J. Liu. Mining smart card data for transit riders' travel patterns. *Transportation Research Part C: Emerging Technologies*, Vol. 36, 2013, pp. 1-12.

[21] Williams, M. J., R. M. Whitaker, and S. M. Allen. Measuring individual regularity in human visiting patterns. In *Privacy, Security, Risk and Trust (PASSAT), 2012 International Conference on and 2012 International Conference on Social Computing (SocialCom)*, IEEE, 2012. pp. 117-122.

[22] Girvan, M., and M. E. Newman. Community structure in social and biological networks. *Proceedings of the national academy of sciences*, Vol. 99, No. 12, 2002, pp. 7821-7826.

[23] Newman, M. E., and M. Girvan. Finding and evaluating community structure in networks. *Physical review E*, Vol. 69, No. 2, 2004, p. 026113.

[24] Radicchi, F., C. Castellano, F. Cecconi, V. Loreto, and D. Parisi. Defining and identifying communities in networks. *Proceedings of the National Academy of Sciences of the United States of America*, Vol. 101, No. 9, 2004, pp. 2658-2663.

[25] Palla, G., I. Derényi, I. Farkas, and T. Vicsek. Uncovering the overlapping community structure of complex networks in nature and society. *Nature*, Vol. 435, No. 7043, 2005, pp. 814-818.

[26] Soundarajan, S., and C. Gomes. Using community detection algorithms for sustainability applications. In *Proceedings of the 3rd International Conference on Computational Sustainability*, 2012.

[27] Lin, L., Q. Wang, and A. Sadek. Data mining and complex network algorithms for traffic accident analysis. *Transportation Research Record: Journal of the Transportation Research Board*, No. 2460, 2014, pp. 128-136.

[28] Wikipedia. *Applications of artificial intelligence*. https://en.wikipedia.org/wiki/Applications_of_artificial_intelligence - Transportation.

[29] Schmidhuber, J. Deep learning in neural networks: An overview. *Neural networks*, Vol. 61, 2015, pp. 85-117.

[30] Gers, F. A., N. N. Schraudolph, and J. Schmidhuber. Learning precise timing with LSTM recurrent networks. *Journal of machine learning research*, Vol. 3, No. Aug, 2002, pp. 115-143.

[31] Fernández, S., A. Graves, and J. Schmidhuber. An application of recurrent neural networks to discriminative keyword spotting. *Artificial Neural Networks-ICANN 2007*, 2007, pp. 220-229.

[32] Krizhevsky, A., I. Sutskever, and G. E. Hinton. Imagenet classification with deep convolutional neural networks. In *Advances in neural information processing systems*, 2012. pp. 1097-1105.

[33] He, K., X. Zhang, S. Ren, and J. Sun. Deep residual learning for image recognition. In *Proceedings of the IEEE conference on computer vision and pattern recognition*, 2016. pp. 770-778.

1 [34] IMAGENET. *Large Scale Visual Recognition Challenge 2016*. [http://image-
2 net.org/challenges/LSVRC/2016/results](http://image-net.org/challenges/LSVRC/2016/results).

3 [35] Dong, W., J. Li, R. Yao, C. Li, T. Yuan, and L. Wang. Characterizing driving styles with deep
4 learning. *arXiv preprint arXiv:1607.03611*, 2016.

5 [36] Kang, C., X. Ma, D. Tong, and Y. Liu. Intra-urban human mobility patterns: An urban morphology
6 perspective. *Physica A: Statistical Mechanics and its Applications*, Vol. 391, No. 4, 2012, pp.
7 1702-1717.

8 [37] Wikipedia. *Jaccard index*. https://en.wikipedia.org/wiki/Jaccard_index.

9 [38] Blondel, V. D., J.-L. Guillaume, R. Lambiotte, and E. Lefebvre. Fast unfolding of communities in
10 large networks. *Journal of statistical mechanics: theory and experiment*, Vol. 2008, No. 10, 2008,
11 p. P10008.

12 [39] TensorFlow. *TensorFlow*. <https://www.tensorflow.org/>.

13

14

1	Table 1 Taxonomy of activity purposes	17
2	Table 2 Activity Purpose Statistics	19
3	Table 3 Statistics of Clusters	20
4	Table 4 Accuracy for traditional machine learning algorithm and CNN.....	21
5		

1	Figure 1 ROG plot	22
2	Figure 2 Distributions of (a) first trip departure time and (b) last trip return time	23
3	Figure 3 Activity maps.....	24
4	Figure 4 The layout of a CNN.....	25
5	Figure 5 Clustering results.....	26
6		
7		

1 **Table 1 Taxonomy of activity purposes**

Activity Purpose Category	Activity Purpose
Home	Personal activities (sleeping, personal care, leisure, chores)
	Preparing meals/eating
	Hosting visitors/entertaining guests
	Exercise (with or without equipment) / playing sports
	Study / schoolwork
	Work for pay at home using telecommunications equipment
	Using computer / telephone / cell or smartphone or other communications device for personal activities
	All other activities at my home
Work	Work / job duties
	Training
	Meals at work
	Work-sponsored social activities (holiday or birthday celebrations, etc.)
	All other work-related activities at my work
	Work-related (meeting, sales call, delivery)
School	In school / classroom / laboratory
	Meals at school / college
	After school or non-class-related sports / physical activity
	All other after school or non-class related activities (library, band rehearsal, clubs, etc.)
Transportation / Transitions (Transit))	Change type of transportation / transfer (walk to bus, walk to / from parked car)
	Pickup / drop off passenger(s)
	Loop trip (for interviewer only-not listed on diary)
Shopping / Errands (Shop)	Routine shopping (groceries, clothing, convenience store, household maintenance)
	Shopping for major purchases or specialty items (appliance, electronics, new vehicle, major household repairs)
	Household errands (bank, dry cleaning, etc.)
Personal Business (Personal)	Volunteer work / activities
	Drive through other (ATM, bank)
	Service private vehicles (gas, oil, lube, repairs)
	Personal business (visit government office, attorney, accountant)
	Healthcare (doctor, dentist, eye care, chiropractic)
Recreation / Entertainment (Rec)	Non-work related activities (social clubs, etc.)
	Exercise / sports

	Drive through meals (snacks, coffee, etc.)
	Eat meal at restaurant / diner
	Outdoor exercise (playing sports / jogging, bicycling, walking, waking the dog, etc.)
	Indoor exercise (gym, yoga, etc.)
	Entertainment (movies, watch sports, etc.)
	Social / visit friends / relatives
Other	Other (specify) [Note: listed on diary)
Other	Don't know / refused

1
2

1 **Table 2 Activity Purpose Statistics**

Activity purpose	Weekday		Weekend	
	Number of Activity	Proportion	Number of Activity	Proportion
Home	199554	54.33%	85920	57.16%
Work	35424	9.64%	4051	2.70%
School	12410	3.38%	381	0.25%
Transit	42142	11.47%	11258	7.49%
Shop	24774	6.75%	14998	9.98%
Person	15299	4.17%	8440	5.62%
Rec	34766	9.47%	24036	15.99%
Other	2911	0.79%	1222	0.81%
Total	367280	100.00%	150306	100.00%

2
3

1 **Table 3 Statistics of Clusters**

Activity purpose	Cluster1		Cluster2		Cluster3		Cluster4		Cluster5		Cluster6	
	# of Activities	Percentage	#	%	#	%	#	%	#	%	#	%
Home	2201	55.74%	545	56.83%	3426	48.53%	548	54.69%	377	56.61%	311	56.75%
Work	37	0.94%	5	0.52%	1936	27.43%	285	28.44%	183	27.48%	1	0.18%
School	1	0.03%	1	0.10%	1	0.01%	0	0.00%	0	0.00%	155	28.28%
Transit*	351	8.89%	51	5.32%	696	9.86%	61	6.09%	35	5.26%	36	6.57%
Shop	650	16.46%	71	7.40%	347	4.92%	46	4.59%	24	3.60%	12	2.19%
Person [#]	234	5.93%	24	2.50%	143	2.03%	15	1.50%	12	1.80%	8	1.46%
Rec	465	11.78%	260	27.11%	504	7.14%	44	4.39%	34	5.11%	24	4.38%
Other	10	0.25%	2	0.21%	6	0.08%	3	0.30%	1	0.15%	1	0.18%

2 * Transit is the abbreviation of “Transportation/Transitions” as mentioned in Table 1.

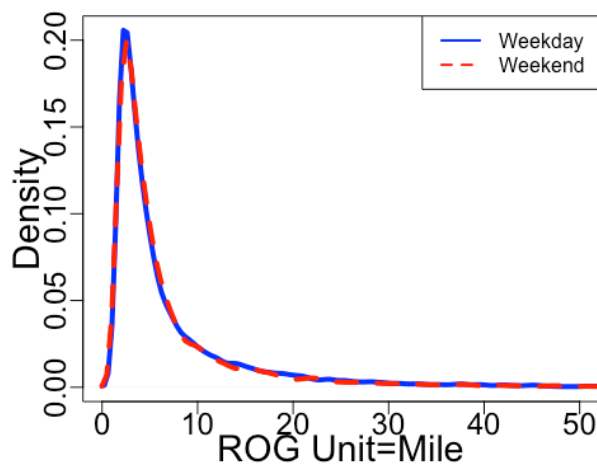
3 [#] Person is the abbreviation of “Personal Business” as mentioned in Table 1.

4

1 **Table 4 Accuracy for traditional machine learning algorithm and CNN**

	SVM	KNN	RF	CNN
Cluster 1	97.5%	100.0%	97.5%	100.0%
Cluster 2	57.5%	87.5%	60.0%	95.0%
Cluster 3	95.0%	90.0%	92.5%	97.5%
Cluster 4	90.0%	97.5%	90.0%	100.0%
Cluster 5	97.5%	97.5%	100.0%	97.5%
Cluster 6	92.5%	100.0%	95.0%	95.0%
Cluster 7	17.5%	35.0%	30.0%	85.0%
Average Accuracy	78.2%	86.8%	80.7%	95.7%

2



1
2 **Figure 1 ROG plot**

3

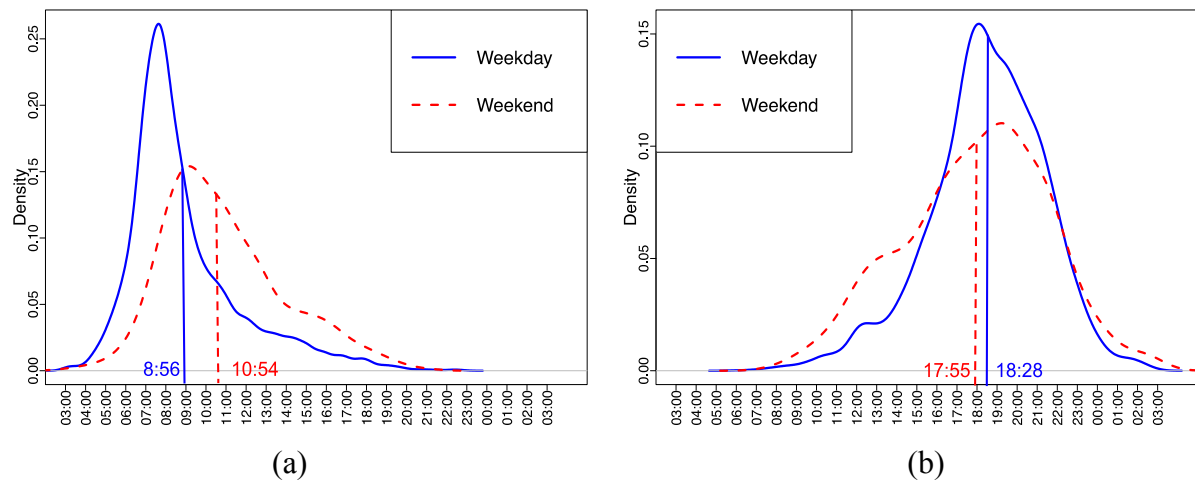
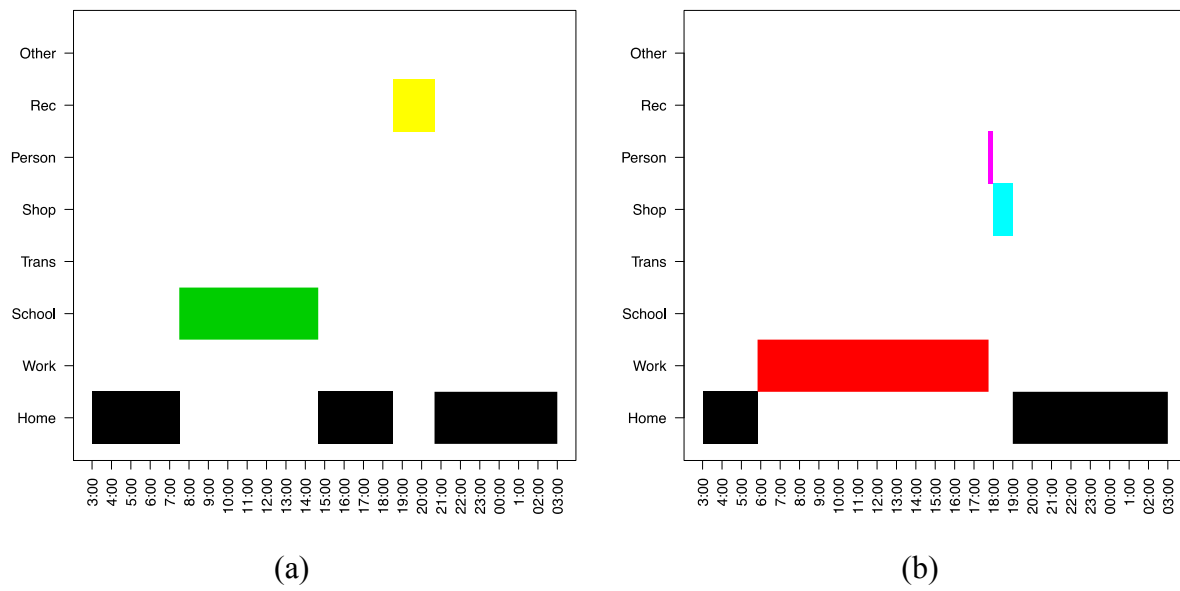
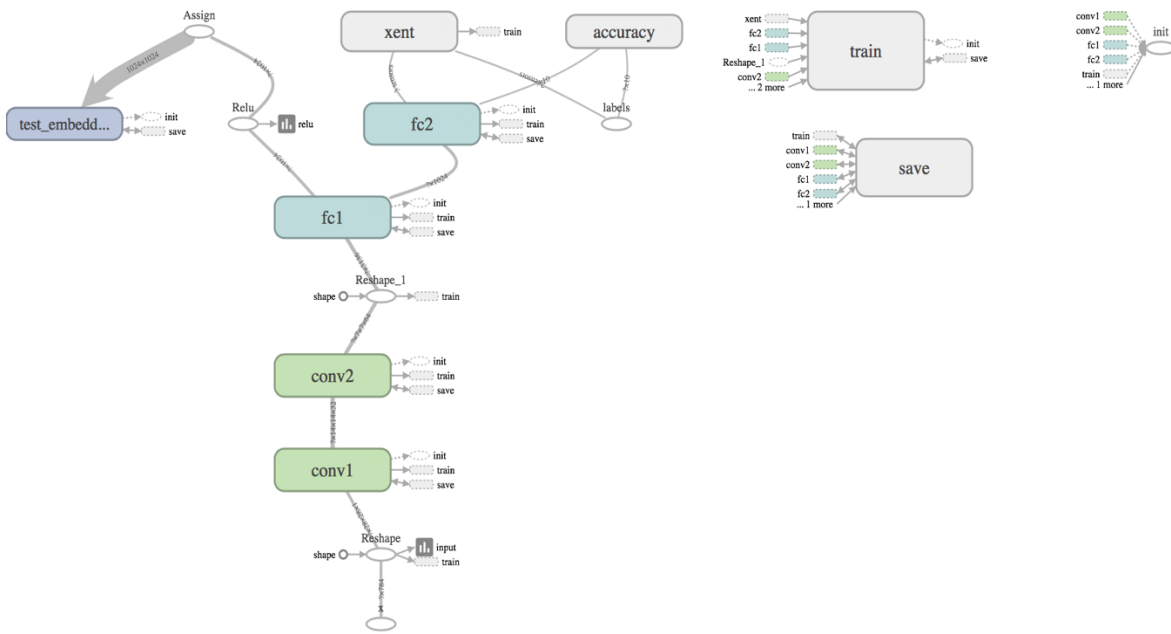


Figure 2 Distributions of (a) first trip departure time and (b) last trip return time



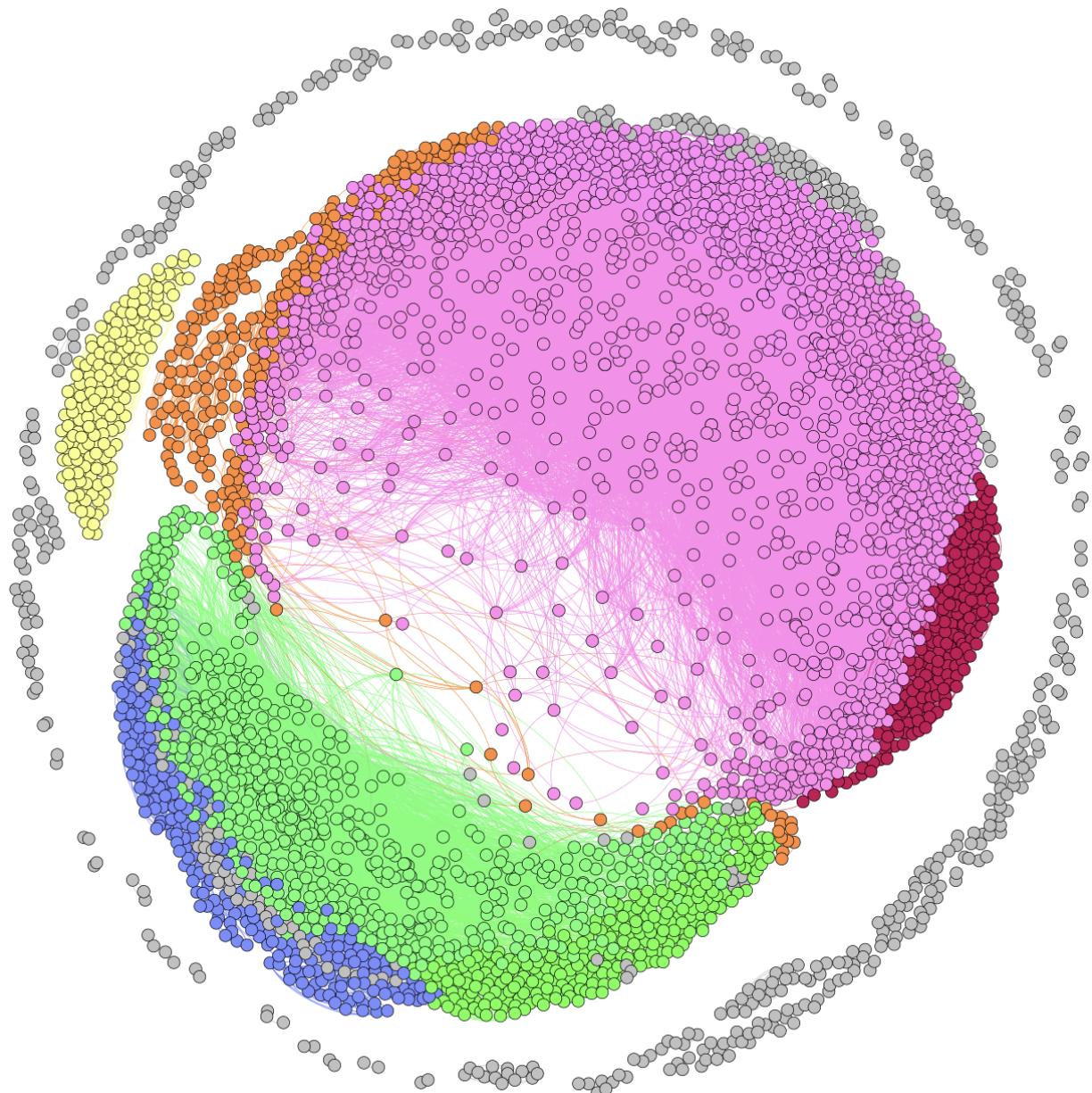
1
2
3
4

Figure 3 Activity maps



1
2 **Figure 4 The layout of a CNN**

3



1
2 **Figure 5 Clustering results**

3
4